ACS OMEGA

http://pubs.acs.org/journal/acsodf

Article

Fabrication of Wet-Spun Wool Keratin/Poly(vinyl alcohol) Hybrid Fibers: Effects of Keratin Concentration and Flow Rate

Oyunkhorol Bayanmunkh, Boldbaatar Baatar, Nomin Tserendulam, Khongorzul Boldbaatar, Chinzorig Radnaabazar, Tegshjargal Khishigjargal, Erdene Norov, and Boldbaatar Jambaldorj*

Cite This: *ACS Omega* 2023, 8, 12327−12333

Read Online

ACCESS | Metrics & More | Article Recommendations | Supporting Information

ABSTRACT: Sheep wool is one of the most common wastes derived from agriculture and also a great source of keratin. In this study, chemical reduction and alkali hydrolysis methods of extracting keratin from wool were studied for the purpose of reusing the waste wool, and the products were used to fabricate wet-spun hybrid fibers by mixing with PVA. The comparative yield of the two extraction methods was investigated, and the optimal precursor concentration ratio for keratin extraction was identified. The effects of keratin concentration and wet-spinning flow rate on the mechanical properties of fabricated fibers were studied. Therefore, this study encourages the further investigation of wool keratin-based hybrid biomaterials, which could provide a new way to reuse waste wool.

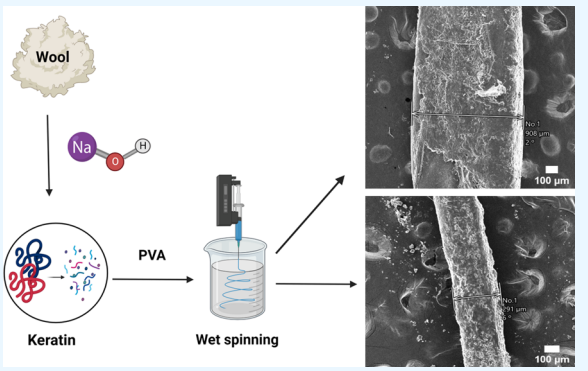

1. INTRODUCTION

Animal husbandry is one of the largest fields of Mongolian agriculture. It is estimated that in Mongolia, 36.7 thousand tons of sheep wool was reserved each year, of which 36.2% was used to manufacture 10 types of products such as carpet and textiles in 2020.[1] The report shows that each passing year, sheep wool reserves keep increasing, which leads to a valuable agricultural resource going to waste.[2]

About 95% of sheep wool is composed of keratin.[3] Keratin is a natural polymer with the potential to be used for various biomedical applications, including cosmetics,[4] medical membranes,[5] bone grafting,[6,7] injectable hydrogel[8−10] and drug delivery.[11−13] Various methods were formerly developed to extract keratin using urea,[14] peracetic acid,[15] sodium hydroxide,[16] sodium bisulfide, ammonium sulfate,[17] and so forth.

Keratin is relatively water-insoluble; therefore, it is usually mixed with other polymers to produce fibers. Keratin fibers blended with poly(vinyl alcohol) (PVA),[18,19] polyamide(lactic acid) (PLA),[20] poly(ethylene oxide),[21−23] poly(ε-caprolactone),[24] poly(lactic-co-glycolic acid) (PLGA),[25] chitosan,[26] gelatin,[27] and hydroxypropyl cellulose[28] have been produced mostly by using electrospinning techniques. However, electrospinning is a preferred method for fabricating membranes of fibrous mesh rather than nanofibers. On the other hand, wet-spun keratin fibers are much less studied. Jin et al.[29] have shown that wet-spun polymer fibers tend to have better thermal stability and mechanical properties than electrospun fibers as the macromolecules in the fibers are organized more uniformly, resulting in a higher proportion of crystallization.

Poly(vinyl alcohol) (PVA) is a good additive for keratin-based fibers to be used in many industries, such as textile industry, paper industry, and food packaging industry because of its thermal stability, low manufacturing cost, nontoxicity, and biodegradable property.[30] However, with the wet-spun fibers made with PVA and S-sulfo keratin[31] in different coagulation baths,[32] the effect of flow rate in the wet-spinning process at room temperature is not investigated extensively in the aforementioned studies.

In this study, keratin was extracted from sheep wool using two distinct methods, and the yield was compared. Furthermore, the extracted keratin was used as a precursor to fabricate the hybrid fibers of keratin/PVA using the wet-spinning method. To emphasize the effect of keratin content and flow rate on the structure and characteristics of hybrid fibers, their properties were characterized by scanning electron microscopy (SEM), Fourier transform infrared spectroscopy (FTIR), and Young's modulus measurements.

2. EXPERIMENTAL METHODS

2.1. Materials. Sheep wool was commercially obtained from a wool textile company (Uguuj-Shim LLC), Mongolia.

Received: January 3, 2023
Accepted: March 9, 2023
Published: March 20, 2023

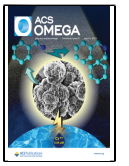

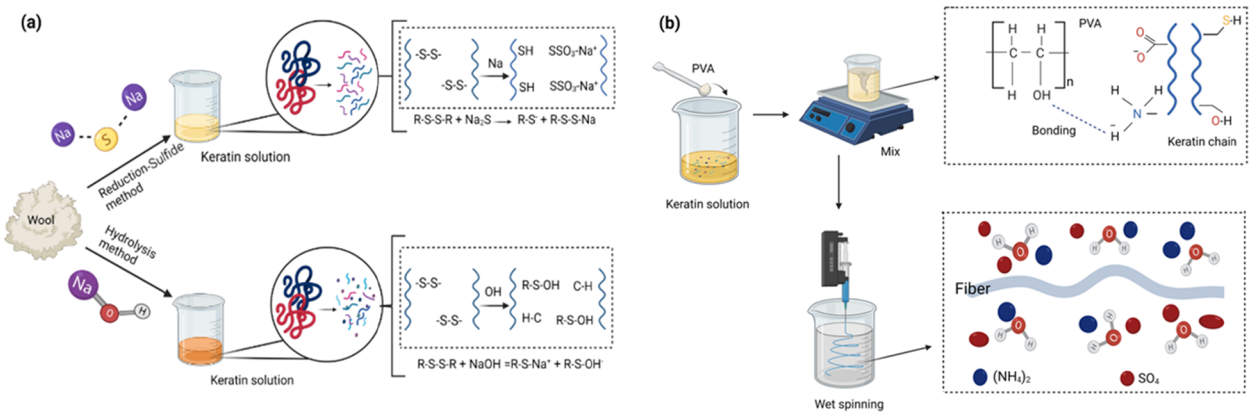

Figure 1. Keratin extraction process schemes using chemical reduction−−sulfide and alkali hydrolysis methods (a) and illustration of the fiber fabrication process by wet-spinning (b).

Analytical grade sodium sulfide nonahydrate ($Na_2S{\cdot}9H_2O$), sodium hydroxide (NaOH), calcium oxide (CaO), hydrochloric acid (HCl), and poly(vinyl alcohol) (PVA-124) with a hydrolyzation degree of ≥97% were bought from Xilong Scientific Co., Ltd., China.

2.2. Keratin Extraction. The keratin extraction and fiber formation processes are illustrated in Figure 1. In the chemical reduction method, the disulfide bonds in wool are broken using long-term exposure to sodium sulfide. In comparison, the hydrolysis method cleaves the disulfide bonds by the rapid action of hydroxide ions at a high temperature, as presented in Figure 1a. While producing a mixture of keratin and PVA, an intermolecular bond between the hydroxide group of PVA and the amino group of keratin was formed. Then, during the wet-spinning process, ammonium and sulfide ions attract and remove water molecules from the keratin/PVA mixture to solidify the fibers, as shown in Figure 1b.

2.2.1. Chemical Reduction−−Sulfide Method. The method of Feairheller et al.[33] for the extraction of cattle hair was adapted as follows. First, wool fibers (1 g) were soaked in 150 mL of deionized water for 20 min; then, 1 g sodium sulfide was added for 5 min, followed by 3.2 g calcium oxide (lime). The mixture was gently stirred for 48 h. 1 g sheep wool was soaked in 60 mL of distilled water under constant stirring at room temperature for 20 min. Then, sodium sulfide (20, 40, 60, and 80 wt % of the wool used) was mixed with the wool sample under constant agitation for 5 min. Afterward, 3.2 g calcium oxide was added to the mixture and left at room temperature for 72 h. Finally, the mixture was filtered using Whatman filter paper and dialyzed for 72 h to purify the extracted keratin.[33,43] Henceforth, the samples extracted by this method are labeled "KCR".

2.2.2. Alkali Hydrolysis Method. 1 g sheep wool was added in 50 mL of sodium hydroxide of varying concentrations (1, 2, 3, and 4 M) and magnetically stirred at 80 °C until the wool dissolved completely. Afterward, the mixture was cooled to room temperature, and concentrated hydrochloric acid was added dropwise into the solution until the pH was in the range 13−7. Finally, the solution was washed by centrifugation at 10,000 rpm for 15 min and dialyzed for 72 h to remove any impurities.[3,34] The samples obtained by this method are labeled "KAH" in this research. Both extraction experiments were performed in triplicates.

2.3. Preparation of PVA/Keratin Blended Solution. For the preparation of a blended solution, PVA was dissolved in distilled water at 121 °C at the ratio of 1:20 (w/w) by an autoclave process. Then, the PVA solution was cooled down to 40°C[35] for blending with various amounts of keratin solution. The PVA/keratin solutions were prepared with keratin contents of 5, 10, and 20% to study the effects of keratin concentration. To fully mix the PVA/keratin solution, the mixed solution was first stirred at 40 °C for 2 h and then placed still for 3 h.

2.4. Preparation of PVA/Keratin Hybrid Fibers. Keratin extracted utilizing the method with the greatest yield was further used for fiber fabrication. PVA/keratin fibers were prepared by the wet-spinning method[23,36] using a self-made coagulation bath. 2 mL of PVA/keratin solution was filled in a 5 mL syringe, and the prefilled syringe was placed to a syringe pump. The PVA/keratin blended solution from the syringe pump was solidified in a coagulation bath that was filled with saturated ammonium sulfate. Then, the hybrid fibers were compressed with three different speeds (10, 20, and 40 mL/h).

2.5. Bradford Protein Assay. The amount of protein extracted by the chemical reduction and alkali hydrolysis methods was determined by the colorimetric method of Bradford using differing concentrations of BSA (0.2, 0.4, 0.6, 0.8, and 1.0 mg/mL). Briefly, 5 mL of Bradford reagent was added to each 100 mcg standard solution in a microfuge tube and incubated at room temperature for 5−20 min.[37] Finally, the absorbance values were measured at 595 nm using a UV−vis spectrophotometer (Shimadzu UV-1650PC, Japan). The protein yield was averaged over three experiments, and the standard deviation was calculated.

The yield of each extraction method was calculated by the ratio between the Bradford sample (Y') and the initial Bradford solution (Y) using the following equation

$$\text{Yield}\ (\%) = \frac{Y \times C}{Y'} \tag{1}$$

2.6. SDS-PAGE Analysis. SDS-PAGE was performed using 20 mcg of the sample reagent in each gel plate using Coomassie blue staining solution.[38] The gel electrophoresis was performed with 20 μL of the protein.

2.7. Surface and Spectral Characterization. The surface topograph of PVA/keratin hybrid fibers was observed with scanning electron microscopy (JCM-6000 PLUS). The chemical composition of keratin, PVA, and PVA/keratin hybrid fibers was characterized by Fourier transform infrared

https://doi.org/10.1021/acsomega.3c00028
ACS Omega 2023, 8, 12327−12333

spectroscopy (Shimadzu, IR Prestige 21, Japan) in the wavenumber region of 500−4000 cm^{-1}.

2.8. Thermal Analysis. The thermal properties of keratin, PVA, and blended fibers of keratin/PVA were evaluated by a thermogravimetry−differential thermal analysis (TG-DTA8122, Rigaku, Japan) system. About 6.5 ±1.5 mg of the sample was placed in an aluminum pan, and temperatures were probed in the range between room temperature and 500 °C at a heating rate of 6 °C/min, in a flowing nitrogen atmosphere at 10 mL/min.

2.9. Young's Modulus. The length of the fiber (strain) under stress was tested by a tensile strength tester (HD-B609B-S, Haida, China). This is widely used in wires, cables, hardware, rubber, leather, apparel, fabric, and tape paper products and measures with an accuracy of 0.001 mm at room temperature.

Young's modulus describes the relative stiffness of a material, which is measured by the elastic slope of a stress and strain graph. Young's modulus was calculated by the ratio of the stress value to its corresponding strain value. If a hybrid fiber of cross-sectional area S is pulled by a force F at each end, the fiber stretches from the original length L_0 to a new length L_1.[39]

$$E = \frac{\text{stress}}{\text{strain}} = \frac{\sigma}{\varepsilon} = \frac{FL_0}{S(L_1 - L_0)} \quad (2)$$

3. RESULTS AND DISCUSSION

3.1. Keratin Extraction Yield. The total protein yields of the different extraction methods are shown in Table 1. The

Table 1. Protein Yield of the Different Extraction Methods

extraction method	concentration (M)	protein yield (M)
reduction	0.008	60.8 ± 0.4
	0.015	64.6 ± 1.2
	0.024	61.5 ± 0.2
	0.031	60.5 ± 0.2
alkali hydrolysis	0.5	30.3 ± 5.1
	1.0	71.3 ± 0.7
	2.0	69.7± 0.3
	4.0	48.0 ± 1.0

KCR extraction yield was 60.8, 64.6, 61.5, and 60.5%, respectively (Figure 2a). In this method, the usage of 0.015 M sodium sulfide produced the highest keratin extraction yield, and increasing the concentration further resulted in a decrease of protein yield.

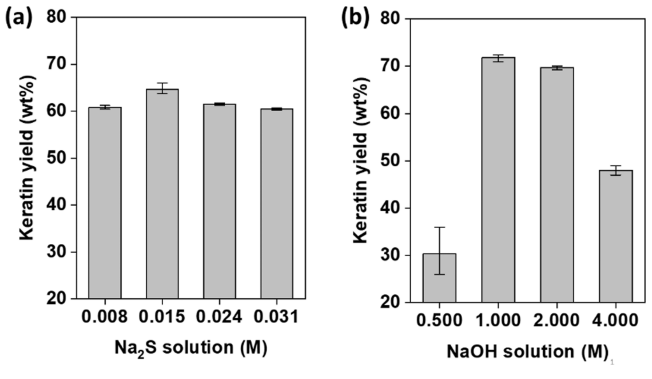

Figure 2. Extraction yields of (a) KCR and (b) KAH.

On the other hand, the KAH extraction yield was 30.3, 71.3, 69.7, and 48% respectively, using 1, 2, 3, and 4 M solutions of sodium hydroxide (Figure 2b). The keratin protein yield was the highest when 1 M solution was used, and a further increase of sodium hydroxide affected the protein yield negatively. In both methods, no significant bands were formed on the SDS-PAGE patterns due to the formation of fragments of different lengths (Supporting Information S1 and S2).

3.2. FT-IR Spectra. The changes in the chemical structure observed through FT-IR spectroscopy for sheep wool, keratin, blended solution, and hybrid fiber composites with different ratios are shown in Figure 3. The results of FT-IR measurements differ by several peaks in the spectra of wool and keratin at 500−4000 cm^{-1}.

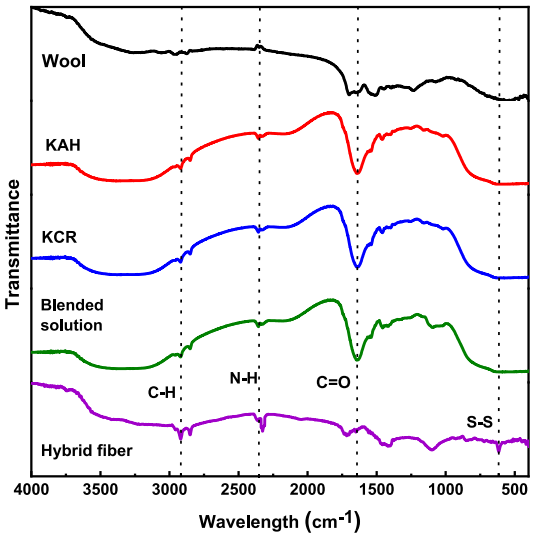

Figure 3. FTIR spectra of wool, KAH, KCR, blended solution, and the keratin/PVA hybrid fiber.

For the spectra of keratin (KAH and KCR), the absorption bands at 2357 and 1631 cm^{-1} are the characteristic amide peaks of amide I and II, respectively.[44] Also, the amide absorption band of mainly the C═O group (1650−1670 cm^{-1}) is observed. The peak at 2357 cm^{-1} corresponds to the bending vibration of N−H coupled with the stretching vibration of C−N of amide II. The absorption peaks at 1631 and S−S 600−620 cm^{-1} are attributed, respectively, to the asymmetric and symmetric S−O stretching vibrations of the cysteine-S-sulfonated residues, which are formed from the reaction of sulfites and cysteine during the protein extraction process. The amine groups and other peaks observed in the spectra of the extracted keratin were similar to Wang et al.'s report of rabbit hair keratin.[40]

Moreover, there is barely any bonding observed in keratin and PVA in liquid state. The bonding process between keratin and PVA was related to the wet-spinning process in which the salt-out process interfered with the intermolecular bonding between the protein amine groups and hydroxyl groups of water, causing the bond formation of amine groups with the hydroxyl and carbonyl groups of PVA. This hypothesis is derived from the observation that the amine peaks on the FT-IR spectra of hybrid fibers had more intensity than on other samples.[41,42]

3.3. Morphology of Hybrid Fibers. The surface images of PVA/keratin hybrid fibers produced with different

https://doi.org/10.1021/acsomega.3c00028
ACS Omega 2023, 8, 12327−12333

concentrations and flow rates are shown in Figure 4. The surface of the fibers is cylindrical with some grooves. The salt

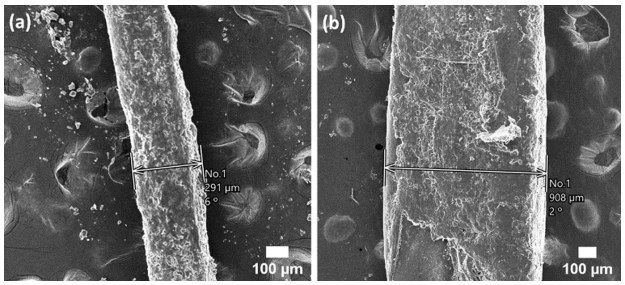

Figure 4. Surface SEM images of hybrid fibers at different flow rates and various contents of keratin: (a) 291 μm, 10 mL/h, 20%; (b) 908 μm, 40 mL/h, 40%.

residues of ammonium sulfate from the coagulation bath were observed as small particles on the fiber (Supporting Information S3).

The average diameters of the fibers are shown in Table 2. The fiber diameter increased with a faster flow rate, as the

Table 2. Relationship between Young's Modulus, Keratin Concentration, and Flow Rate

concentration of keratin (%)	flow rate (mL/h)	average diameter (μm)	Young's modulus (MPa)
5	10	203±13	27.2 ± 7.7
	20	469±13	8.4±0.3
	40	614±20	3.4 ± 2.9
10	10	225±24	19.1 ± 2.5
	20	618±24	4.5 ± 1.2
	40	849±11	1.1 ± 0.1
20	10	291±5	20.9 ± 12.11
	20	366±12	7.74 ± 6.30
	40	576±9	3.75 ± 0.59
40	10	405±5	8.31 ± 2.64
	20	663±10	2.86 ± 1.55
	40	908±11	1.39 ± 0.41

additional fluid pumped out of the syringe added to the thickness of the fiber. Generally, the fibers produced with the lowest concentration of keratin (5 wt %) with the lowest flow rate (10 mL/h) were the thinnest, and vice versa.

3.4. Thermal Analysis. Thermal analysis is an efficient way of monitoring the mass change versus the increasing temperature. The mass loss due to the thermal process was determined by thermogravimetric analysis and the peak degradation of keratin, PVA, and keratin/PVA hybrid fibers (20 mL/h); the analysis was conducted at a heating rate of 6 °C/min under nitrogen atmosphere.

As shown in Figure 5a, two weight loss stages were observed in the keratin TG curves. The first weight loss corresponding to the moisture vaporization of water occurred below 220 °C, and the second one taking place above 270 °C involved the decomposition of keratin molecules. Tsuchiya and Sumi[45] reported that after the water molecules are eliminated from the PVA chain at 245 °C, it forms a conjugated polyene structure. Meanwhile, three weight loss peaks are observed in the TG curve for PVA. The first (97 °C) and second (200 °C) ones were similar to keratin. The last and major stage above 220 °C was due to the thermal degradation and by-product formation

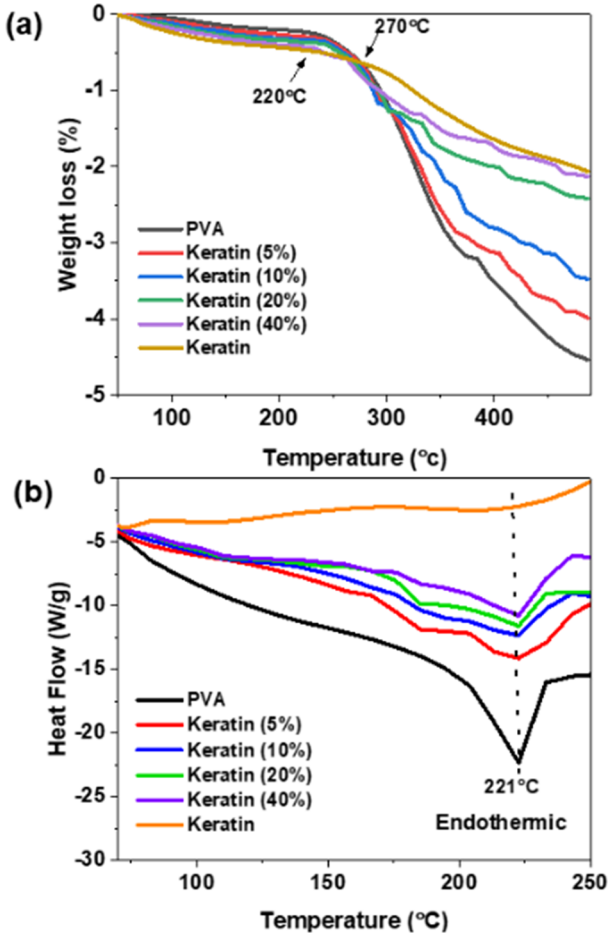

Figure 5. Representative TG (a) and DTA (b) curves of keratin, PVA, and hybrid fibers with various concentrations of keratin.

of PVA during thermal degradation.[46] Compared to the TG curves of keratin and PVA, it is observed that keratin has a higher onset temperature and higher weight residue of thermal degradation than PVA and therefore higher thermal stability. Furthermore, as the amount of keratin in the hybrid fiber rises, it takes on characteristics that align with pure keratin, whereas as the keratin content diminishes, it starts to resemble PVA. Figure 5b shows the DTA curves of keratin, PVA, and hybrid fibers with various concentrations of keratin. It was worth noting that the DTA curves of all samples were with obvious endothermic peaks, and the intensities of hybrid fibers were between those of keratin and PVA, which is in agreement with the TGA curves. A relatively large and sharp endothermic peak is observed at about 221 °C and is assigned to the melting temperature of pure PVA, which agrees with the reported data.[46,47] This peak gradually shifts the melting temperature to a larger value. This is because the majority of the hybrid fibers have the fiber diameter increased with a faster flow rate state due to the rapid solidification process of stretched fibers during wet-spinning. Meanwhile, the endothermic peak that occurred below 220 °C was mainly caused by the evaporation of water, which took place above 270 °C, resulting from the thermal decomposition of materials. Also, compared to keratin and PVA, it is observed that keratin has a higher onset temperature and a higher weight residue of thermal degradation.

3.5. Young's Modulus. As shown in Figure 6, Young's modulus was inversely proportional to the fiber diameter.

https://doi.org/10.1021/acsomega.3c00028
ACS Omega 2023, 8, 12327−12333

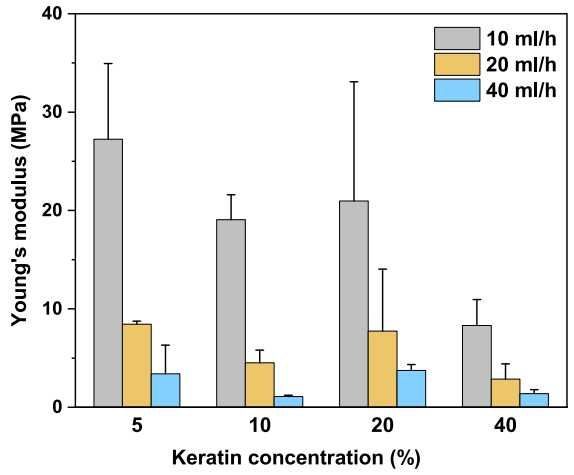

Figure 6. Young's module measurement comparisons depending on the keratin concentration in hybrid fibers and the flow rate.

Therefore, thinner fibers generally had higher Young's modulus and were more resistant to strain. Meanwhile, Young's modulus decreased as the diameter increased, and the fiber became elongated. This is due to the low salt-out process in the center of the fiber. As the fiber gets thicker, the salt-out process becomes unable to penetrate into the middle of the fiber. Consequently, the thicker fibers were easily elongated.

4. CONCLUSIONS

In this study, keratin was successfully extracted using reduction−−sulfide and alkali hydrolysis methods. The keratin/PVA fibers were prepared by wet-spinning, and their structure, width, and elasticity were investigated. The alkali hydrolysis method using 1 M NaOH showed the biggest yield of keratin. SDS-PAGE results have shown that keratin fibers were extracted as protein fractions. FT-IR analyses of keratin by the two extraction methods were similar, with the peaks corresponding to the peptide chains, amine groups, and other functional groups of the protein. Intermolecular bonding between the −NH group of keratin and −OH group of PVA was observed in the FT-IR analysis. As the speed of the salt-out process remains constant, the diameter of hybrid fibers was directly related to the flow rate because the increased flow rate causes more fluid to pump out without giving it enough time to solidify. Furthermore, the thermal analysis was directly related to the concentration of keratin, and the Young's modulus was inversely proportional to the diameter of the fibers.

■ ASSOCIATED CONTENT

Supporting Information

The Supporting Information is available free of charge at https://pubs.acs.org/doi/10.1021/acsomega.3c00028.

Protein data (Bradford assay and SDS-PAGE) and the surface SEM images of hybrid fibers (PDF)

■ AUTHOR INFORMATION

Corresponding Author

Boldbaatar Jambaldorj − *Center of Nanoscience and Nanotechnology, Department of Chemical and Biological Engineering and Applied Science, National University of Mongolia, Ulaanbaatar 14200, Mongolia;* orcid.org/0000-0002-7256-3780; Email: Boldbaatar.j@seas.num.edu.mn

Authors

Oyunkhorol Bayanmunkh − *Center of Nanoscience and Nanotechnology, Department of Chemical and Biological Engineering and Applied Science, National University of Mongolia, Ulaanbaatar 14200, Mongolia*

Boldbaatar Baatar − *Center of Nanoscience and Nanotechnology, Department of Chemical and Biological Engineering and Applied Science, National University of Mongolia, Ulaanbaatar 14200, Mongolia*

Nomin Tserendulam − *Center of Nanoscience and Nanotechnology, Department of Chemical and Biological Engineering and Applied Science, National University of Mongolia, Ulaanbaatar 14200, Mongolia*

Khongorzul Boldbaatar − *Center of Nanoscience and Nanotechnology, Department of Chemical and Biological Engineering and Applied Science, National University of Mongolia, Ulaanbaatar 14200, Mongolia; Leather Study Department, Research and Development Institute of Light Industry, Mongolian University of Science and Technology, Ulaanbaatar 14191, Mongolia*

Chinzorig Radnaabazar − *Department of Chemical and Biological Engineering and Applied Science, National University of Mongolia, Ulaanbaatar 14200, Mongolia*

Tegshjargal Khishigjargal − *Center of Nanoscience and Nanotechnology, Department of Chemical and Biological Engineering and Applied Science, National University of Mongolia, Ulaanbaatar 14200, Mongolia*

Erdene Norov − *Center of Nanoscience and Nanotechnology, Department of Chemical and Biological Engineering and Applied Science, National University of Mongolia, Ulaanbaatar 14200, Mongolia*

Complete contact information is available at: https://pubs.acs.org/10.1021/acsomega.3c00028

Author Contributions

O.B. and B.B. equally contributed to the study by carrying out the extraction of keratin and completed the fabrication of hybrid fibers.

Funding

This work has received funding from National University of Mongolia under grant agreement (P2021-4194), and Science and Technology Foundation of Mongolia (Project No: ShUSs-2018/48).

Notes

The authors declare no competing financial interest.

■ ACKNOWLEDGMENTS

The authors thank Dr. Odgerel Oidomsambuu (Laboratory of Genetic Engineering, National University of Mongolia) for assistance with equipment.

■ REFERENCES

(1) *Report of sheep wool production*; Ministry of Food, Agriculture and Light Industry: Mongolia, 2020.

(2) Sun, Y.; Li, B.; Zhang, Y.; Dou, H.; Fan, W.; Wang, S. The progress and prospect for sustainable development of waste wool resources. *Text. Res. J.* **2023**, *93*, 468−485.

(3) Shavandi, A.; Bekhit, A. E.-D. A.; Carne, A.; Bekhit, A. Evaluation of keratin extraction from wool by chemical methods for bio-polymer application. *J. Bioact. Compat. Polym.* **2017**, *32*, 163−177.
(4) Burnett, C. L.; Bergfeld, W. F.; Belsito, D. V.; Hill, R. A.; Klaassen, C. D.; Liebler, D. C.; Marks, J. G., Jr.; Shank, R. C.; Slaga, T. J.; Snyder, P. W.; Gill, L. J.; Heldreth, B. Safety Assessment of Keratin and Keratin-Derived Ingredients as Used in Cosmetics. *Int. J. Toxicol.* **2021**, *40*, 36S−51S.
(5) Carvalho, C. R.; Costa, J. B.; Costa, L.; Silva-Correia, J.; Moay, Z. K.; Ng, K. W.; Reis, R. L.; Oliveira, J. M. Enhanced performance of chitosan/keratin membranes with potential application in peripheral nerve repair. *Biomater. Sci.* **2019**, *7*, 5451−5466.
(6) Dias, G. J.; Mahoney, P.; Hung, N. A.; Sharma, L. A.; Kalita, P.; Smith, R. A.; Kelly, R. J.; Ali, A. Osteoconduction in keratin−hydroxyapatite composite bone-graft substitutes. *J. Biomed. Mater. Res. B Appl. Biomater.* **2017**, *105*, 2034−2044.
(7) Dias, G. J.; Ramesh, N.; Neilson, L.; Cornwall, J.; Kelly, R. J.; Anderson, G. M. The adaptive immune response to porous regenerated keratin as a bone graft substitute in an ovine model. *Int. J. Biol. Macromol.* **2020**, *165*, 100−106.
(8) Sharma, A.; Lavanya; Love, R. M.; Ali, M. A.; Sharma, A.; Macari, S.; Avadhani, A.; Dias, G. J. Healing Response of Rat pulp Treated with an Injectable Keratin Hydrogel. *J. Appl. Biomater. Funct. Mater.* **2017**, *15*, e244−e250.
(9) Tang, A.; Li, Y.; Yao, Y.; Yang, X.; Cao, Z.; Nie, H.; Yang, G. Injectable keratin hydrogels as hemostatic and wound dressing materials. *Biomater. Sci.* **2021**, *9*, 4169−4177.
(10) Xu, S.; Zhang, C.; Zhang, A.; Wang, H.; Rao, H.; Zhang, Z. Fabrication and biological evaluation in vivo of an injectable keratin hydrogel as filler materials. *J. Bioact. Compat. Polym.* **2016**, *31*, 179−190.
(11) Cilurzo, F.; Selmin, F.; Aluigi, A.; Bellosta, S. Regenerated keratin proteins as potential biomaterial for drug delivery. *Polym. Adv. Technol.* **2013**, *24*, 1025−1028.
(12) Li, Q.; Zhu, L.; Liu, R.; Huang, D.; Jin, X.; Che, N.; Li, Z.; Qu, X.; Kang, H.; Huang, Y. Biological stimuli responsive drug carriers based on keratin for triggerable drug delivery. *J. Mater. Chem.* **2012**, *22*, 19964−19973.
(13) Perotto, G.; Sandri, G.; Pignatelli, C.; Milanesi, G.; Athanassiou, A. Water-based synthesis of keratin micro- and nanoparticles with tunable mucoadhesive properties for drug delivery. *J. Mater. Chem. B* **2019**, *7*, 4385−4392.
(14) Liu, R.; Li, L.; Liu, S.; Li, S.; Zhu, X.; Yi, M.; Liao, X. Structure and properties of wool keratin/poly (vinyl alcohol) blended fiber. *Adv. Polym. Technol.* **2018**, *37*, 2756−2762.
(15) Shavandi, A.; Carne, A.; Bekhit, A. A.; Bekhit, A. E.-D. A. An improved method for solubilisation of wool keratin using peracetic acid. *J. Environ. Chem. Eng.* **2017**, *5*, 1977−1984.
(16) Sinkiewicz, I.; Śliwińska, A.; Staroszczyk, H.; Kołodziejska, I. Alternative Methods of Preparation of Soluble Keratin from Chicken Feathers. *Waste Biomass Valoriz.* **2017**, *8*, 1043−1048.
(17) Gupta, A.; Kamarudin, N. B.; Kee, C. Y. G.; Yunus, R. B. M. Extraction of Keratin Protein from Chicken Feather. *J. Chem. Chem. Eng.* **2012**, *6*, 732−737.
(18) He, M.; Zhang, B.; Dou, Y.; Yin, G.; Cui, Y.; Chen, X. Fabrication and characterization of electrospun feather keratin/poly(vinyl alcohol) composite nanofibers. *RSC Adv.* **2017**, *7*, 9854.
(19) Li, S.; Yang, X.-H. Fabrication and Characterization of Electrospun Wool Keratin/Poly(vinyl alcohol) Blend Nanofibers. *Adv. Mater. Sci. Eng.* **2014**, *2014*, No. e163678.
(20) Isarankura Na Ayutthaya, S.; Tanpichai, S.; Sangkhun, W.; Wootthikanokkhan, J. Effect of clay content on morphology and processability of electrospun keratin/poly(lactic acid) nanofiber. *Int. J. Biol. Macromol.* **2016**, *85*, 585−595.
(21) Aluigi, A.; Varesano, A.; Montarsolo, A.; Vineis, C.; Ferrero, F.; Mazzuchetti, G.; Tonin, C. Electrospinning of keratin/poly(ethylene oxide)blend nanofibers. *J. Appl. Polym. Sci.* **2007**, *104*, 863−870.
(22) Yong, L.; Jia, L.; Jie, F.; Meng, W. Preparation and characterization of electro spun human hair keratin/poly (ethylene oxide) composite nanofibers. *Matéria (Rio J.)* **2014**, *19*, 382.
(23) Ma, H.; Shen, J.; Cao, J.; Wang, D.; Yue, B.; Mao, Z.; Zhang, H. Fabrication of wool keratin/polyethylene oxide nano-membrane from wool fabric waste. *J. Clean. Prod.* **2017**, *161*, 357−361.
(24) Edwards, A.; Jarvis, D.; Hopkins, T.; Pixley, S.; Bhattarai, N. Poly(ε-caprolactone)/keratin-based composite nanofibers for biomedical applications. *J. Biomed. Mater. Res. B Appl. Biomater.* **2015**, *103*, 21−30.
(25) Zhang, H.; Wang, J.; Ma, H.; Zhou, Y.; Ma, X.; Liu, J.; Huang, J.; Na, Y. Bilayered PLGA/Wool Keratin Composite Membranes Support Periodontal Regeneration in Beagle Dogs. *ACS Biomater. Sci. Eng.* **2016**, *2*, 2162.
(26) Islam, M. T.; Laing, R. M.; Wilson, C. A.; McConnell, M.; Ali, M. A. Fabrication and characterization of 3-dimensional electrospun poly(vinyl alcohol)/keratin/chitosan nanofibrous scaffold. *Carbohydr. Polym.* **2022**, *275*, No. 118682.
(27) Yao, C.-H.; Lee, C.-Y.; Huang, C.-H.; Chen, Y.-S.; Chen, K.-Y. Novel bilayer wound dressing bSased on electrospun gelatin/keratin nanofibrous mats for skin wound repair. *Mater. Sci. Eng. C* **2017**, *79*, 533−540.
(28) Cao, G.; Rong, M. Z.; Zhang, M. Q. Continuous High-Content Keratin Fibers with Balanced Properties Derived from Wool Waste. *ACS Sustainable Chem. Eng.* **2020**, *8*, 18148−18156.
(29) Jin, S.; Chen, Z.; Xin, B.; Xi, T.; Meng, N. An investigation on the comparison of wet spinning and electrospinning: Experimentation and simulation. *Fibers Polym.* **2017**, *18*, 1160−1170.
(30) Du, H.; Liu, W.; Zhang, M.; Si, C.; Zhang, X.; Li, B. Cellulose nanocrystals and cellulose nanofibrils based hydrogels for biomedical applications. *Carbohydr. Polym.* **2019**, *209*, 130−144.
(31) Katoh, K.; Shibayama, M.; Tanabe, T.; Yamauchi, K. Preparation and properties of keratin−poly(vinyl alcohol) blend fiber. *J. Appl. Polym. Sci.* **2004**, *91*, 756−762.
(32) Xu, H.; Yang, Y. Controlled De-Cross-Linking and Disentanglement of Feather Keratin for Fiber Preparation via a Novel Process. *ACS Sustainable Chem. Eng.* **2014**, *2*, 1404−1410.
(33) Feairheller, S. H.; Taylor, M. M.; Windus, W.; Filachione, E. M.; Naghski, J. Recovery and analyses of hair proteins from tannery unhairing wastes. *J. Agric. Food Chem.* **1972**, *20*, 668−670.
(34) Zhang, Z.; Zhang, X.; Nie, Y.; Wang, H.; Zheng, S.; Zhang, S. Effects of water content on the dissolution behavior of wool keratin using 1-ethyl-3-methylimidazolium dimethylphosphate. *Sci. China Chem.* **2017**, *60*, 934−941.
(35) Hassan, C. M.; Trakampan, P.; Peppas, N. A. Water Solubility Characteristics of Poly(vinyl alcohol) and Gels Prepared by Freezing/Thawing Processes. in *Water Soluble Polymers: Solutions Properties and Applications* ed. Amjad, Z.; Springer US, 2002, 31−40.
(36) Ozipek, B.; Karakas, H. Wet spinning of synthetic polymer fibers. In *Advances in filament yarn spinning of textiles and polymers*; Woodhead Publishing, 2014, 174−186.
(37) Bradford, M. M. A rapid and sensitive method for the quantitation of microgram quantities of protein utilizing the principle of protein-dye binding. *Anal. Biochem.* **1976**, *72*, 248−254.
(38) Sambrook, J.; Russell, D. W. *Molecular cloning: a laboratory manual*; Cold Spring Harbor Laboratory, 2001.
(39) Kraemer, F.; Roellig, M.; Metasch, R.; Ahmar, J.; Meier, K.; Wiese, S. Experimental determination of the Young's modulus of copper and solder materials for electronic packaging. *Microelectron. Reliab.* **2018**, *91*, 251−256.
(40) Wang, X.; Shi, Z.; Zhao, Q.; Yu, Y. Study on the structure and properties of biofunctional keratin from rabbit hair. *Materials* **2021**, *14*, 379.
(41) Chen, X.; Wu, S.; Yi, M.; Ge, J.; Yin, G.; Li, X. Preparation and Physicochemical Properties of Blend Films of Feather Keratin and Poly(vinyl alcohol) Compatibilized by Tris(hydroxymethyl)-aminomethane. *Polymer* **2018**, *10*, 1054.
(42) Choo, K.; Ching, Y. C.; Chuah, C. H.; Julai, S.; Liou, N.-S. Preparation and Characterization of Polyvinyl Alcohol-Chitosan

https://doi.org/10.1021/acsomega.3c00028
ACS Omega 2023, 8, 12327−12333

Composite Films Reinforced with Cellulose Nanofiber. *Materials (Basel)* **2016**, *9*, No. 644.
(43) Brown, E. M.; Pandya, K.; Taylor, M. M.; Liu, C. K. Comparison of methods for extraction of keratin from waste wool. *Agric. Sci.* **2016**, *07*, 670.
(44) Nandiyanto, A. B.; Oktiani, R.; Ragadhita, R. How to read and interpret FTIR spectroscope of organic material. *Indones. J. Sci. Technol.* **2019**, *4*, 97−118.
(45) Tsuchiya, Y.; Sumi, K. Thermal decomposition products of poly(vinyl alcohol). *J. Polym. Sci., Part A-1: Polym. Chem.* **1969**, *7*, 3151−3158.
(46) Islam, M. S.; Karim, M. R. Fabrication and characterization of poly(vinyl alcohol)/alginate blend nanofibers by electrospinning method. *Colloids Surf.* **2010**, *366*, 135.
(47) Lee, J. S.; Choi, K. H.; Ghim, H. D.; Kim, S. S.; Chun, D. H.; Kim, H. Y.; Lyoo, W. S. Role of molecular weight of atactic poly(vinyl alcohol) (PVA) in the structure and properties of PVA nanofabric prepared by electrospinning. *J. Appl. Polym. Sci.* **2004**, *93*, 1638−1646.

https://doi.org/10.1021/acsomega.3c00028
ACS Omega 2023, 8, 12327−12333